Title:

Incorporating Ligament Laxity in the Upper Cervical Spine for Finite Element Modeling

Author Names and Affiliations:

Timothy L Lasswell[a], Duane S Cronin[a], John B Medley[a], Parham Rasoulinejad[b]

[a]Department of MME, University of Waterloo, 200 University Avenue West, Waterloo, Canada

[b]Victoria Hospital, London Health Sciences Center, 800 Commisioners Road East, London, Canada

Submitted to: The Spine Journal

Corresponding Author: Duane S Cronin
Department of Mechanical Engineering
University of Waterloo
200 University Ave. West
Waterloo, Ontario, Canada, N2L 3G1
dscronin@mecheng1.uwaterloo.ca
(519) 888-4567 x32682

Abstract

Background Context:

Predicting physiological range of motion (ROM) using a finite element (FE) model of the upper cervical spine requires the incorporation of ligament laxity. The effect of ligament laxity can only be observed on a macro level of joint motion and is lost once ligaments have been dissected and preconditioned for experimental testing. As a result, ligament laxity values are not directly available in the literature for use in FE models.

Purpose:

The purpose of the current study it to propose an optimization process that can be used to determine a set of ligament laxity values for upper cervical spine FE models. Furthermore, an FE model that includes ligament laxity will be analyzed against experimental data for physiological ROM as well as experimental data for the increase in ROM when a type II odontoid fracture is introduced.

Study Design/Setting:

The upper cervical spine FE model was adapted from a fiftieth percentile male full body model developed with the Global Human Body Models Consortium (GHMBC). FE modeling was performed in LS-DYNA (Livermore Software Technology Group, Livermore CA) and LS-OPT (Livermore Software Technology Group, Livermore CA) was used for ligament laxity optimization.

Methods:

Ordinate-based curve matching was used to minimize the mean squared error (MSE) between computed load-rotation curves and experimental load-rotation curves under flexion, extension and axial rotation with pure moment loads from 0-3.5Nm. Lateral bending was excluded from the optimization since the upper cervical spine is primarily responsible for flexion, extension and

axial rotation. Based on recommendations from the literature, four varying inputs representing laxity in select ligaments were optimized in order to minimize the MSE. Funding was provided by the Natural Sciences and Engineering Research Council of Canada as well as GHMBC. There are no conflicts of interest to be reported.

Results:

The MSE was reduced to 0.28 in the FE model with optimized ligament laxity compared to an MSE 0f 4.16 in the FE model without laxity. In all load cases, incorporating ligament laxity improved the agreement between the ROM of the FE model and the ROM of the experimental data. The ROM for axial rotation and extension was within one standard deviation of the experimental data. The ROM for flexion and lateral bending was outside one standard deviation of the experimental data but a compromise was required in order to use one set of ligament laxity values to achieve a best fit to all load cases. After a type II odontoid fracture was incorporated into the model, the increase in ROM was in good agreement with experimental data from the literature.

Conclusions:

The optimization approach used in this study provided values for ligament laxities that, when incorporated into the FE model, improved the ROM response when compared to experimental data. Successfully modeling a type II odontoid fracture showcased the robustness of the FE model which can now be used in future biomechanics studies.

Keywords: Ligament laxity; Upper cervical spine; Finite element modeling; range of motion; Atlantoaxial instability; Odontoid; Optimization

Classifications: Technical Report

Introduction

FE modeling can be done to examine the mechanical behavior of the upper cervical spine, particularly when it is instrumented with fusion constructs[1]. Generating realistic results from an upper cervical spine FE model requires selection of appropriate ligament laxities because even when fusion constructs are in place, ligaments play a significant role in the kinematics and dynamics in this region.

The native kinematics of vertebral segments C2-C3 through to C6-C7 are similar in the sense that motion is constrained by cervical discs between the vertebral bodies, articular facet joints and the posterior osteoligamentous complex. However, the native motion of the occipital-atlanto-axial joint (C012) significantly differs from the rest of the cervical spine, most notably because 50% of axial rotation of the cervical spine occurs at the atlanto-axial joint[2]. To accommodate these large range of motions, the boney structures of C012 are held together by ligaments with considerable laxity[3,4].

Atlantoaxial instability (AAI) occurs when there is excessive movement at the first two vertebrae in the cervical spine (C1-C2) that has generally occurred due to inflammatory diseases, degenerative osteoarthritis or cervical spine trauma[5]. The leading cause of AAI is traumatic fracture of the odontoid process, which accounts for 20% of all cervical spine fractures[6]. Odontoid fractures have been classified into three types by Anderson and D'Alonzo[7] depending on the location of the fracture line in the C2 vertebrae. Generally, it is accepted that Type I and Type III fractures be treated conservatively with hard collar immobilization regardless of patient age[8]. Additionally, due to high non-union rates, it is generally recommended that Type II

fractures in non-geriatric patients, who meet the required surgical criteria, be treated with the anterior odontoid screw surgical technique[9]. Controversy arises when it comes to the recommended treatment for geriatric patients suffering from Type II odontoid fractures. The anterior odontoid screw technique is not often used for the geriatric patient population because of low union rates due to osteoporotic bone at the fracture site, risk of postoperative dysphagia requiring surgical intervention and risk of pneumonia[10]. Alternatively, C1-C2 arthrodesis techniques are the surgical treatment of choice for geriatric patients, with the Harms procedure being the gold standard[11]. Even with arthrodesis techniques, only 50% of this geriatric patient population can be treated surgically due to concerns relating to operation time, intraoperative blood loss, invasiveness and recovery time[12].

Several new procedures have been proposed in attempts to increase the number of geriatric patients that can be treated surgically for AAI. Most new procedures suggest using a percutaneous or minimally invasive surgical technique with existing commercial implants[13–15]. However, novel surgical techniques and novel implants that address the unique needs of the C1-C2 anatomy have also been proposed in the hopes of treating more geriatric patients surgically and improving patient outcomes[16–18]. The development of these novel implants has been largely driven by cadaveric range of motion (ROM) studies based on testing protocols established by Goel et al.[4] or Panjabi et al.[19]

More recently, FE modeling has been used in the orthopaedic implant design process and, in particular cases, has been used to model the biomechanical performance of implants intended to treat AAI[1,20–22]. FE modeling is useful in orthopaedic product development because it allows the

kinematics, dynamics and stresses to be analyzed in much more detail than is feasible by manual calculations. Provided it is realistic, accurate and precise, FE modeling allows faster and more cost effective design iterations when compared to traditional laboratory or cadaveric testing. While laboratory and cadaveric testing are still important to validate data from the FE model, the overall time to develop implant designs can be much reduced.

Detailed FE models of the full cervical spine have been used for a wide range of applications including investigations of injury mechanisms sustained during cases of traumatic loading, such as whiplash in a motor vehicle accident[23–26]. However, FE models used in traumatic loading differed from that needed for AAI implant design. Firstly, the FE model needed for AAI implant design must simulate biomechanics over the natural ROM of the upper cervical spine under physiological loads and loading rates. Secondly, the FE model needed to only contain the vertebrae and associated ligaments over C012. External muscle loading could then be simulated by applying boundary conditions that had been proposed in the literature[3]. This allowed the focus of the FE model to be on ROM of C012 under physiological loading.

Previously, a detailed neck FE model consisting of spine segments C0 to C7 was validated for traumatic loading cases[27] and is part of a larger full body FE model developed with the GHMBC[28]. It was found that the C012 complex of the full neck FE model was overly stiff when ligament laxity was not incorporated. As a result, laxities were introduced in select upper cervical spine ligaments and optimized to experimental data at traumatic loading levels[4,29,30].

In the present study, a FE model of the C012 complex was isolated from the GHBMC FE model (Figure 1). The intention was to adapt this FE model to ROM scenarios of typical daily activities rather than traumatic loading cases. In doing so, the ligament laxity values in the FE model had to be determined from experimental ROM data of cadaveric necks. The existence of ligament laxity in the upper cervical spine was well described in the literature and attributed to being responsible for the large ROM that occurred with negligible load, deemed the neutral zone[3,31]. However, determining individual ligament laxities from the experimental data was difficult because published force-displacement data had been obtained from separate experiments in which the specimens were preconditioned. As a result, determining ligament laxities in the current FE model became an exercise in numerical optimization.

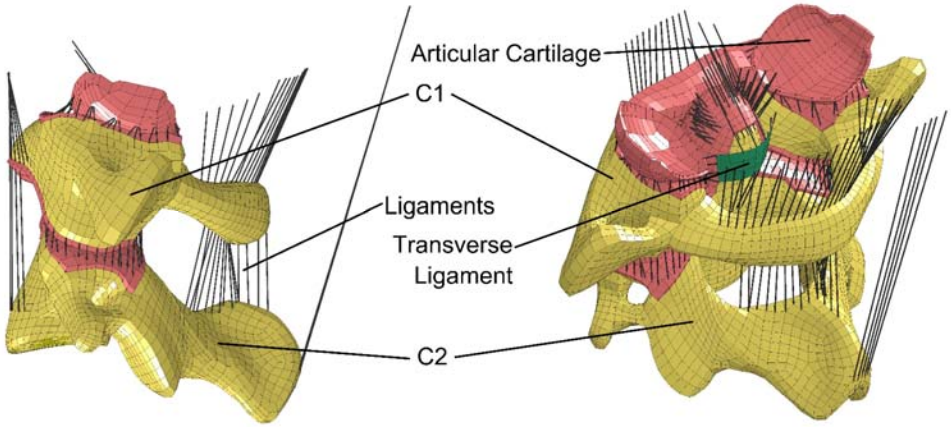

Figure 1: (left) Lateral view of upper cervical spine model and (right) posterolateral view of upper cervical spine model (skull omitted in both views)

Materials and methods

Defining ligament laxity

To establish a baseline, the C012 complex from the existing M50 GHMBC FE model, but excluding ligament laxity, was analyzed under flexion, extension, lateral bending and axial rotation. When compared to experimental ROM data[4,19,29], it was found that the FE model was too stiff in all loading cases when ligament laxity was not incorporated. To better represent the

experimental data, laxities were introduced into select ligaments. Ligament laxity was interpreted to be a lateral shift in the force-displacement curve of each selected ligament (Figure 2). Apart from this lateral shift, the ligament force-displacement curves were implemented using a series of non-linear tension-only elements, following the approach proposed by Panzer et al.[32] and Dewit et al.[33] The total ligament force was divided evenly between the elements. The non-linear ligament force-displacement response was incorporated directly from experimental data[34]. For implementation in the FE model, ligament laxity was defined as the amount of displacement that a ligament could undergo before a force response was generated.

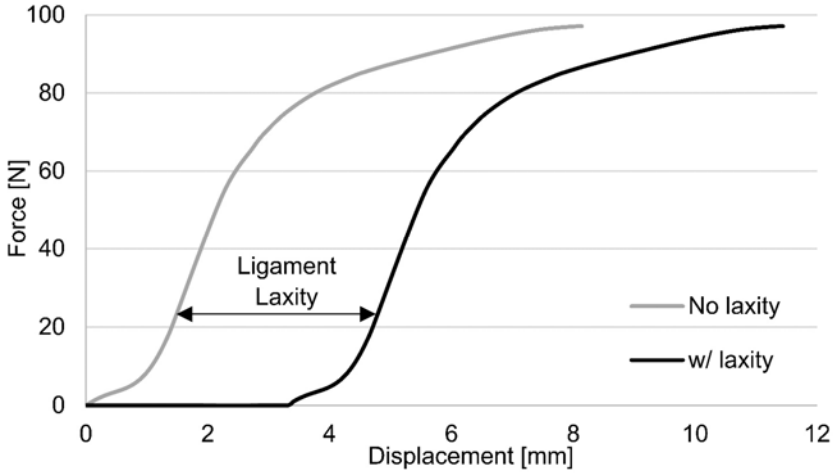

Figure 2: Effect of ligament laxity implementation on the posterior atlanto-axial membrane force-displacement curve

Ligament selection

Based on recommendations from current literature, the following ligaments were selected for laxity optimization (Figure 3): anterior atlanto-axial membrane (AA-AM), posterior atlanto-axial membrane (PA-AM), anterior atlanto-occipital membrane (AA-OM), posterior atlanto-occipital membrane (PA-OM), atlanto-occiptial junction (C0-C1) capsular ligaments (CL01), C1-C2 capsular ligaments (CL12).

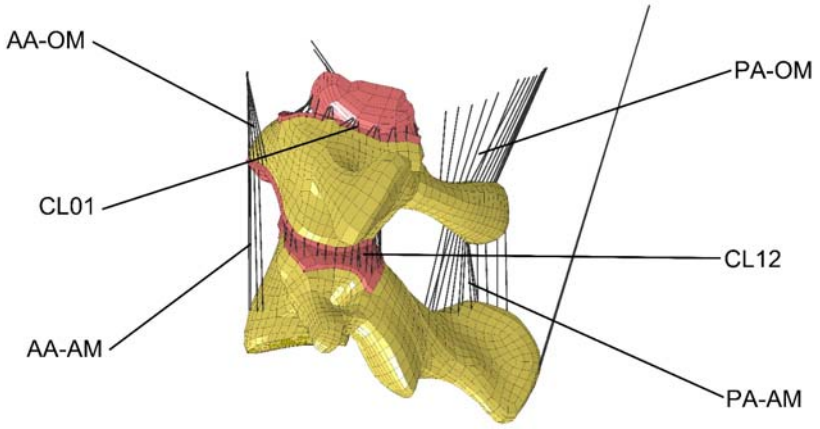

Figure 3: Selected ligaments for laxity optimization

The implementation of laxity into CL12 and CL01 was consistent with experimental data from Panjabi et al. [31,35] who found that the alar ligaments were crucial in restraining axial rotation but the capsular ligaments played only a minor role. This finding suggested that there was laxity in CL12 and CL01 since, if no laxity was present, the moments generated by these ligaments would have restrained motion to a larger degree than the alar ligaments because of a larger lateral distance from the center of rotation.

The membrane ligaments were selected for laxity optimization because being fascial sheets; they were not expected to generate reaction forces that substantially limit motion. Rather, extension of the upper cervical spine is limited by compression of the sub-occipital muscles and flexion is limited by tension in the posterior neck muscles[2]. With no laxity in the membrane ligaments, there would be a larger contribution to restraining the upper cervical spine because the ligaments are located at a significant distance from the center of rotation in the sagittal plane and would therefore create large restraining moments. Selection of these ligaments for laxity optimization also agreed with a study by Shateri et al.[36] where a sensitivity analysis was undertaken to investigate ligament laxities in an upper cervical spine FE model. The findings of their study also

suggested that laxities should be added to the capsular and membrane ligaments across the C012 complex. All other ligaments in the upper cervical spine were not changed in comparison to the baseline and thus were modeled with no laxity.

Optimization process

The FE model was performed using a commercial code (LS-DYNA version R7.1.2, LSTC) and a non-linear optimization software (LS-OPT version 4.2, LSTC) was used to optimize the laxities of the selected ligaments present in C012. The multi-objective function for the optimization was to minimize the MSE between the computed FE model curves and target curves for the following load cases across C012: axial rotation, flexion and extension. Ordinate-based curve matching was used and the MSE represented the discrepancy between the target and computed curves by providing a dimensionless error of the order of unity[37]. Experimental data from Goel et al.[4] was used as the target curve for the axial rotation load case and experimental data from Nightingale et al.[29] were used as the target curves for the flexion and extension cases. To optimize motion of individual segments, additional target curves were developed for C0-C1 motion based on the suggested ratios of C0-C1 motions to the global C012 motions that were presented by Panjabi et al.[31,38]. Boundary conditions were applied as prescribed motion and deformation rate effects were removed from the ligaments to provide boundary conditions that best represented experimental setups. The FE model was also run at half speed and quarter speed and inertial effects were found to be insignificant.

Four variables, representing the laxities of specific ligaments or ligament pairs, were used as inputs into the optimization program. This number of inputs were chosen based on the following

considerations. If laxities between posterior and anterior ligaments at the same level differed largely, then large sagittal head rotations would be present in tensile loading data due to the unequal moment reactions. Therefore, equalizing the laxities of anterior and posterior ligaments was considered to be logical since there was little sagittal head rotation present in the cervical spine when a tensile load was applied in line with the occipital condyles[30]. As a result, the laxities of AA-OM and PA-OM were set equal and the laxities of AA-AM and PA-AM were set equal. Additionally, the properties of the capsular ligaments were set to be laterally symmetric and therefore had the same laxity. This agreed with experimental data which shows no significant difference in right axial rotation and left axial rotation[4,39,40]. Lateral bending motion was also simulated in the FE model of the present study, but ultimately excluded from the optimization process since the upper cervical spine was considered to be primarily responsible for axial rotation and flexion/extension. However, the lateral bending case was still presented for the FE model without ligament laxity and compared to the FE model with optimized ligament laxity. A channel frequency class (CFC) 60 Butterworth filter was applied to the computed curves to remove high frequency oscillations.

A D-Optimal design was used to map the ligament laxity optimization space, with 8 points being evaluated at each iteration. The allowable laxity range for each ligament was determined through several preliminary analyses that helped understand the model response. A linear polynomial model was used to map the optimization surface for each iteration and predict optimal points for the next iteration.

Fracture modeling

Once the converged ligament laxity values were incorporated in the FE model, a type II odontoid fracture was created by deleting the elements at the base of the odontoid (Figure 4). This was representative of experimental setups where the odontoid fracture was often created by transecting the odontoid or performing an odontoidectomy[41]. To determine the increase in motion of the destabilized state, the FE model with the type II fracture was then analyzed under flexion, extension, lateral bending and axial rotation conditions up to a load limit of 1.5Nm, corresponding to the available experimental ROM data. ROM from the FE model was obtained by measuring angles created by four points. Two of the points created a vector on C1 and two of the points created a vector on C2. The angle created between these two vectors at a boundary load of 1.5Nm was then projected onto the plane of motion in the global coordinate system and used as the ROM value. Contact was modelled using a standard penalty-based contact algorithm, but it was noted that contact did not occur in any of the loading cases due to the odontoid distracting away from the vertebral body of C2.

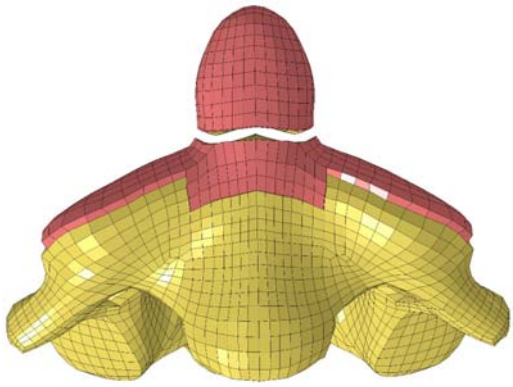

Figure 4: Anterior detail of simulated type II odontoid fracture in FE model

Results

After running the optimization for twenty iterations the ligament laxities had converged to their final values (Table 1). The computed motion curves from the FE model without ligament laxity were stiffer than the experimental curves in all cases. The FE model was in much better agreement with the experimental ROM data after the optimized ligament laxity values were included. With ligament laxity values included, the MSE decreased to 0.28 compared to an initial value of 4.16 in the FE model without ligament laxity.

Table 1: ~~Selected ligaments for optimization~~Allowable range and converged values for ligament laxity optimization process

	CL01	CL12	AA-OM/PA-OM	AA-AM/PA-AM
Minimum allowable value (mm)	0.0	3.0	3.0	2.0
Maximum allowable value (mm)	3.0	6.0	6.0	4.0
Converged value (mm)	1.4	5.4	5.8	3.3

Axial rotation

In axial rotation (Figure 5a), the predicted ROM for the FE model with ligament laxity (40° at 2.47 Nm) was larger than the experimental value from Goel et al.[4] (36.2° at 3.5 Nm). Also, it was observed that the FE model reached the rotational limit of 40° at the termination time of the simulation before the moment could reach 3.5 Nm. However, despite the larger ROM, the FE model with laxity was still in general agreement with the experimental data in that it falls within the ± 1 standard deviation corridor. The addition of ligament laxity in the FE model had a large effect on the ROM when compared with the ROM of the FE model without laxity (24.4° at 3.5 Nm). Over the range of ligament laxities considered, the CL12 ligaments were found to have the largest influence (68%) on the axial rotation MSE. The CL01 ligaments had the second largest influence (27.3%) followed by the membrane ligaments across the C012 complex (combined influence of 4.6%). The MSE between the computed axial rotation curves and the experimental

axial rotation curves was 0.062 when ligament laxity was included compared with an MSE of 0.62 when ligament laxity was not included.

Flexion

In flexion (Figure 5b), the predicted ROM from the FE model with ligament laxity (22.3° at 3.5 Nm) was smaller than the experimental value from Nightingale et al.[29] (30.7° at 3.5 Nm). However, the FE model with ligament laxity presented a more realistic ROM compared with the FE model without laxity (12.4° at 3.5 Nm) even though the FE model with laxity was just outside of the ± 1 standard deviation corridor of the experimental data. Over the range of the ligament laxity considered, the AA-AM/PA-AM ligaments were found to have the largest influence (75.3%) on the flexion MSE. The CL01 ligaments had the second largest influence (16.8%) followed by the CL12 ligaments (4.6%) and the AA-OM/PA-OM ligaments (3.3%). The MSE between the computed flexion curves and the experimental flexion curves was 0.053 when ligament laxity was included in the FE model as opposed to an MSE of 0.51 when ligament laxity was not included. It was also noted that there was a reduction in the moment response of the FE model at approximately 15° of rotation. This reduction was caused by the onset of motion at C1-C2 in the sagittal plane. Before 15° of rotation, the motion had been generated only at C0-C1.

Extension

In extension (Figure 5c), the predicted ROM from the FE model with ligament laxity (3.5 Nm, 24.4°) was in good general agreement with the experimental data from Nightingale et al.[29] (29.6° at 3.5 Nm) falling well within the ±1 standard deviation corridor. Over the range of ligament

laxity considered, the AA-AM/PA-AM ligaments were found to have the largest influence (65.2%) on the extension MSE. The CL01 ligaments had the second largest influence (29.0%) followed by the AA-OM/PA-OM ligaments (5.8%). The CL12 ligaments did not have any influence (0.0%). The MSE between the computed extension curves and the experimental extension curves was 0.16 when ligament laxity was included compared with an MSE of 3.0 when ligament laxity was not included.

Lateral bending

In lateral bending (Figure 5d), the predicted ROM was presented even though the FE model had not been optimized for this loading scenario. The ROM from the FE model with ligament laxity (8.4° at 1.5 Nm) was smaller than the experimental values and outside their ±1 standard deviation corridor. However, the addition of ligament laxity in the FE model did move the predicted ROM much closer to the experimental values[3,38–40] compared with the ROM of the FE model without laxity (4.8° at 1.5 Nm).

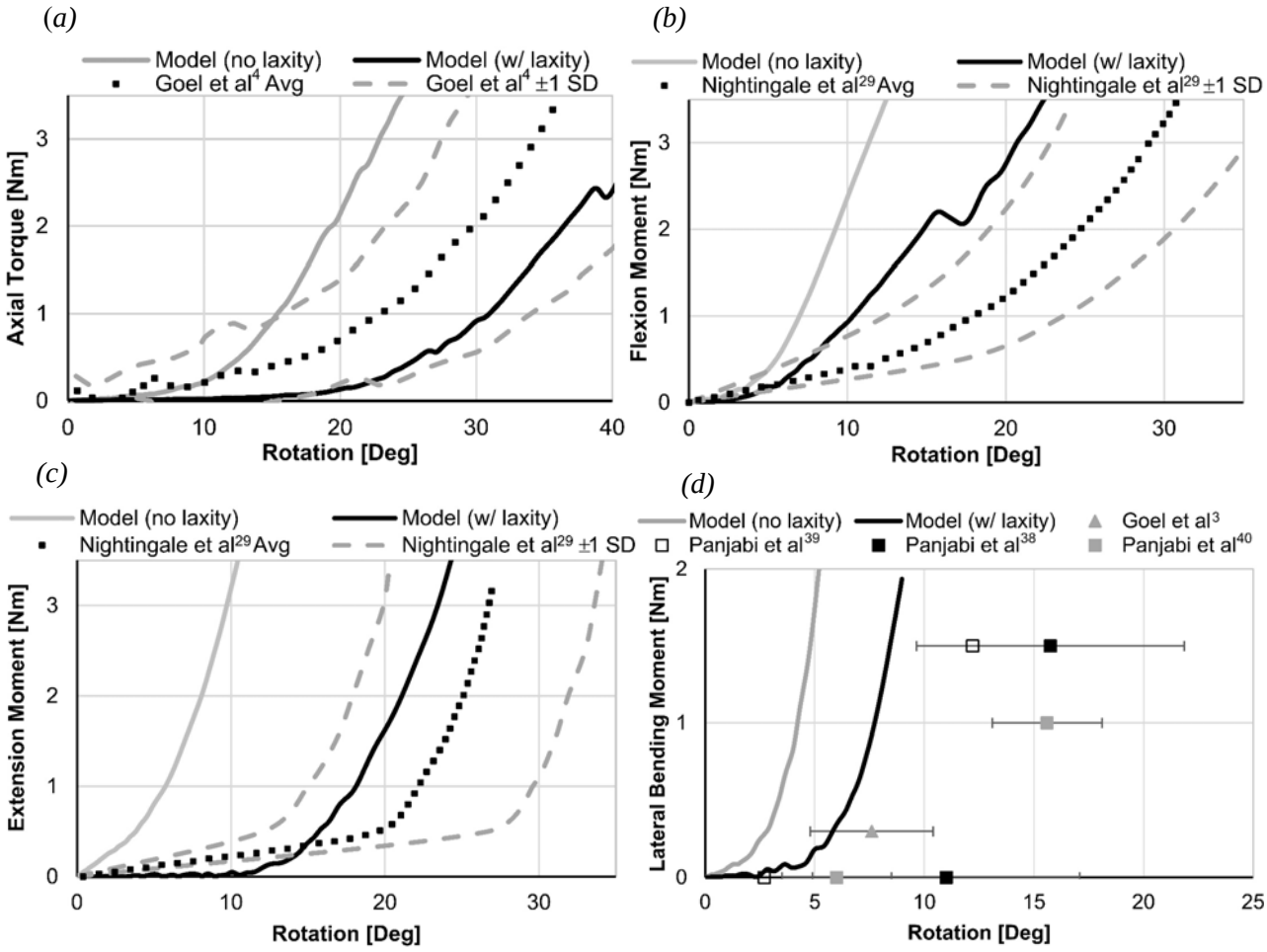

Figure 5: Load rotation curves of C012 motion for (a) axial rotation, (b) flexion, (c) extension and (d) lateral bending

Comparisons to other data

Further comparisons were made with discrete data from Panjabi et al[31,38,39] that did not cover a large enough load range to be used in the optimization (Figure 6). The findings were similar to those presented in Figure 5. There was a much more realistic ROM for the FE model with laxity compared with the FE model without laxity across all modes of loading. The FE model with laxity remained within the ±1 standard deviation corridor for axial rotation and extension. However, the flexion case (Figure 6b) showed a stiffer response than the experimental data with the ROM for the FE model both with and without laxity falling outside the ±1 standard deviation corridor. Lateral bending was omitted from Figure 6 because the data had already been presented in Figure 5d.

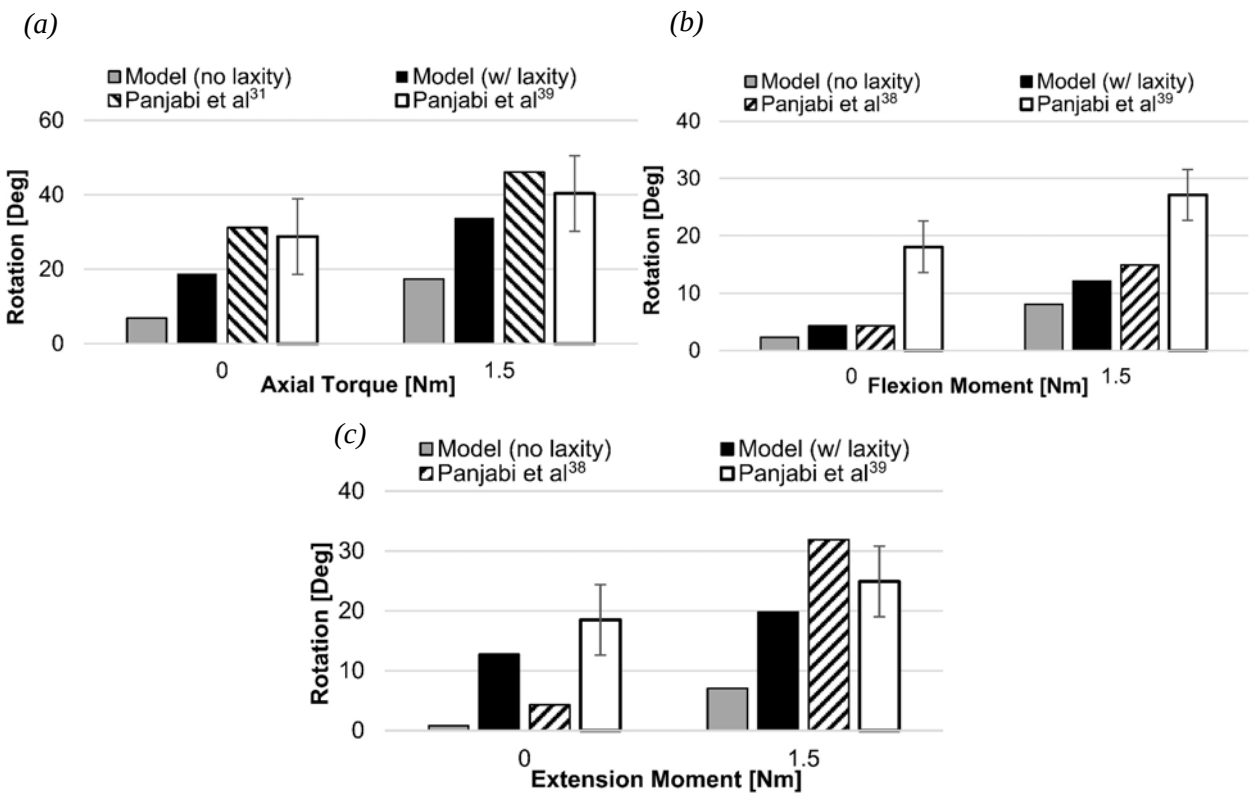

Figure 6: Comparison of FE model ROM for C012 with additional experimental ROM data that was not used for optimization in (a) axial rotation, (b) flexion and (c) extension

Segmental motion

When comparing the segmental level motion of the FE model to experimental data[31,38] (Figure 7), it was found that adding laxity to the FE model predicted segmental motion that was closer to the measured motion of the C012 complex in axial rotation and lateral bending. In axial rotation, the segmental motion ratio went from 27% in the FE model without laxity to 22% in the FE model with laxity compared to the experimental value of 12%. The lateral bending segmental motion ratio was in good agreement with the experimental value of 33% in both FE models but adding laxity did improve the ratio of the FE model from 38% to 34%. For flexion, the segmental motion ratio of the FE model with laxity and the FE model without laxity differed from the experimental value by 8%. However, in the FE model with laxity the segmental motion ratio was 61%, 8% higher than the experimental value as opposed to the FE model without laxity

which was 45%, 8% lower than the experimental value. In extension, the segmental motion ratio decreased to 29% in the FE model with laxity, down from 52% in the FE model without laxity compared to an experimental value of 58%. Extension was the only case where the addition of ligament laxity did not improve the agreement between the FE model response and the experimental data for segmental motion.

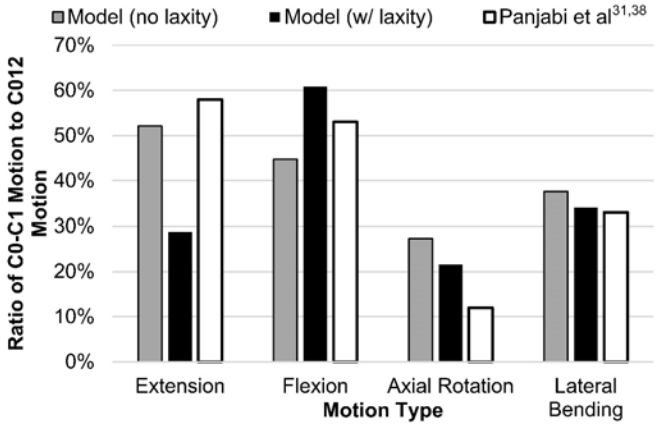

Figure 7: Ratio of C0-C1 rotation to C012 rotation for different types of physiological motion at 1.5 Nm load

Increase in ROM after fracture

When a type II odontoid fracture was simulated in the FE model with ligament laxity, ROM at the C1-C2 level increased in all cases (Table 2). This increase in ROM was within the range of the experimental data from the literature[42–44] (Figure 8). While the scatter in the experimental data is large, the general trend shows that a type II odontoid fracture caused lateral bending to have the largest relative increase in ROM, followed by flexion/extension and axial rotation respectively.

Table 2: C1-C2 motion of FE model with laxity at a load of 1.5 Nm

	FE Intact	FE w/Type II Fracture	% Increase
Flexion/Extension (degrees)	9.3	13.9	49%
Axial Rotation (degrees)	26.7	29.6	11%
Lateral Bending (degrees)	2.5	16.3	546%

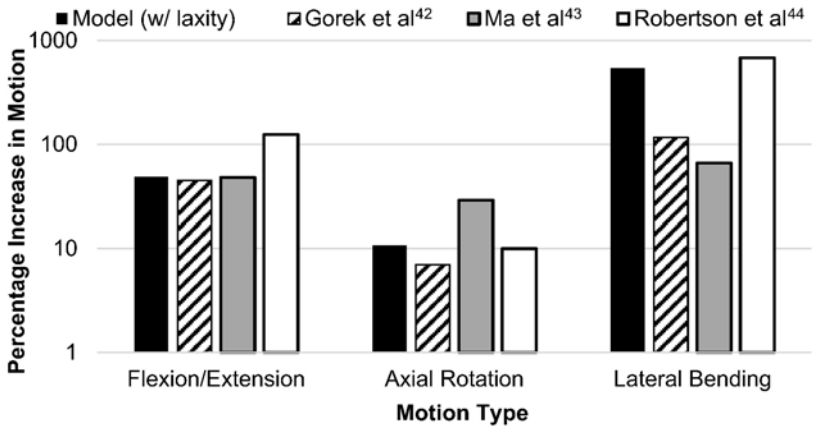

Figure 8: Increase in C1-C2 motion at 1.5 Nm due to a type II odontoid fracture relative to the intact state (log scale used so that the large experimental scatter could be clearly visualized)

When the FE model was run for lateral bending conditions with both the intact and fractured odontoid case, a large amount of coupled axial rotation and coupled extension was identified which resulted in non-planar motion. The ROM calculation method of projecting angles onto planes did not adequately capture this coupled motion so images from the FE model have been given to demonstrate the coupled motion (Figure 9). In the intact case with a load of 1.5 Nm, the most apparent coupled motion was axial rotation. For the fractured odontoid case at 1.5 Nm, coupled axial rotation was still present but coupled extension was also introduced.

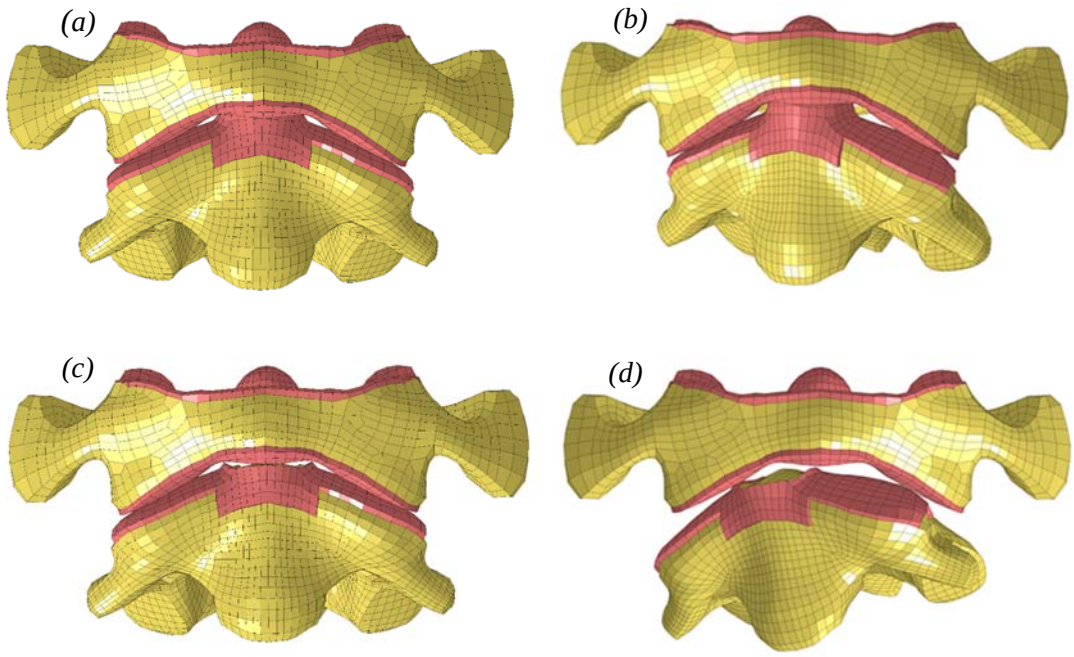

Figure 9: Lateral bending case from FE model with a) intact odontoid at no load, b) intact odontoid at 1.5Nm load, c) fractured odontoid at no load and d) fractured odontoid at 1.5Nm load (ligaments removed from images)

Discussion:

In general, the FE model was able to predict ROM data for upper cervical spine motions under axial rotation, flexion/extension and lateral bending that was in good general agreement with experimental data. Including ligament laxity in the FE model improved the agreement with the experimental data and improved the chances of the FE model predicting clinically realistic average ROM behavior. For the FE model to be physically consistent, a single optimal set of ligament laxities had to be used for all modes of loading. The optimized set of ligament laxities generated load-rotation curves for axial rotation and extension that were within one standard deviation of the experimental data. The load-rotation curves for flexion and lateral bending were deemed to be acceptable even though they were outside one standard deviation of this experimental data.

Closer agreement might not be possible because the experimental data might have bias errors related to the experimental setup, motion capture devices that were used as well as the age and level of degeneration present in the cadaveric specimens. Additionally, some fidelity was lost in the experimental data since only the average ROM curves were reported. It was not known whether any of the individual specimens exhibited motion that was close to the average ROM in all modes of loading. The large standard deviation in the experimental data suggested that this may not have been the case and in reality a specimen that closely replicates the average ROM curves might not exist. Individual ROM curves from the experimental data might also differ in shape compared to the average curve. For example, in flexion the FE model predicted a drop in the resultant moment once motion began at the C1-C2 segment. This drop might also be present in some of the experimental curves but due to the variability in the data could have been filtered out once averaging was performed.

Overall, analyzing the sensitivity of each load-rotation curve to changes in ligament laxity gave results that seemed plausible. Changes in the axial rotation load-rotation curve were most influenced by the ligament laxities of the capsular ligaments. This was considered logical because the capsular ligaments were located at the lateral extremes of the C012 complex and therefore created the largest moment restraints in response to axial rotation. More laxity was clearly required at the C1-C2 level due to the majority of axial rotation coming from this level. Conversely, the C0-C1 level allowed very little axial rotation so optimal ligament laxity value for CL01 was much less than CL12. Flexion/extension for C012 motion improved when compared with the experimental data when the ligament laxity values of AA-AM/PA-AM were increased to the upper extreme of the design space. However, this had a negative effect on one of

the optimization objectives which was to maintain realistic motion at the segmental level. Increasing AA-AM/PA-AM laxity resulted in excessive motion at the C1-C2 level which was not realistic. As a result, the flexion/extension optimization was most sensitive to changes in the ligament laxity values for AA-AM/PA-AM. The flexion/extension load-rotation curve was also sensitive to the changes in the laxity value of CL01. Adding laxity to CL01 shifted the flexion/extension load-rotation curves closer to the motion found experimentally. However, increasing laxity in CL01 shifted the axial rotation away from the motion found experimentally. This resulted in the final value of CL01 being a compromise between maximizing flexion and extension while minimizing axial rotation at the C0-C1 level.

The load-rotation predictions of the present FE model were in good general agreement with other experimental data sets that were not used for the optimization. The experimental data from Panjabi et al.[31,38,39] has been commonly used to support the ROM of FE models in other studies[1,21,22] before using them to test novel upper cervical spine implants under the same loading conditions. The decision to optimize the present FE model over a larger load range of 0 Nm to 3.5 Nm was made to ensure that the FE model was well behaved in the load range of 1.5 Nm that was considered to be of interest for future studies using the FE model.

Incorporating a type II odontoid fracture into the laxity optimized FE model increased the ROM by amounts that were consistent with experimental data in the literature. Applying the FE model to the upper cervical spine with an odontoid fracture was important because this condition has been included in cadaveric studies that assess the performance of implants to treat AAI.

It was found that large coupled motions were present when the loading condition corresponding to lateral bending was applied to the FE model. Such coupled motions were also reported experimentally by Panjabi et al.[38] which found coupled motions in extension and axial rotation when testing lateral bending ROM at the C1-C2 level.

Limitations

Some limitations of the current FE model include the anatomy that was used in the model, the absence of laxity in some ligaments and how the odontoid fracture was implemented. The anatomy of the FE model was generated from a single fiftieth percentile male. This optimization study only looked at ligament laxities as varying inputs. In reality, the anatomical geometry also plays a role in the ROM of the upper cervical spine. Furthermore, all of the ligaments in the upper cervical spine were likely to have some laxity and so the FE model was limited by only applying laxity to select ligaments.

Conclusions

A robust FE model of the upper cervical spine has been produced and used to determine the degree of instability caused by a type II odontoid fracture. Future work with the FE model that now has optimized ligament laxities will include biomechanics testing of novel cervical spine implants in comparison to existing implants. This would help streamline the design process of new AAI fusion constructs by reducing the time and cost associated with traditional cadaveric or laboratory testing.

References

1. Puttlitz CM, Goel VK, Traynelis VC, Clark CR. A finite element investigation of upper cervical instrumentation. *Spine (Phila Pa 1976)*. 2001;26(22):2449-2455.
2. Bogduk N, Mercer S. Biomechanics of the cervical spine. I: Normal kinematics. *Clin Biomech*. 2000;15(9):633-648.
3. Goel VK, Clark CM, Gallaes K, Liu YK. Moment-rotation relationships of the ligamentous occipito-atlanto-axial complex. *J Biomech*. 1988;21(8):673-680.
4. Goel VK, Winterbottom JM, Schulte KR, Chang H, Gilbertson LG. Ligamentous laxity across C0-C1-C2 complex. *Spine (Phila Pa 1976)*. 1990;15(10):990-996.
5. Shih Y-T, Kao T-H, Pan H-C, Chen H-T, Tsou H-K. The surgical treatment principles of atlantoaxial instability focusing on rheumatoid arthritis. *Biomed Res Int*. 2015:1-8.
6. Ochoa G. Surgical management of odontoid fractures. *Injury*. 2005;36(2):54-64.
7. Anderson LD, D'Alonzo RT. Fractures of the odontoid process of the axis. *J bone Jt surgery Am*. 1974;56(8):1663-1674.
8. Southwick WO. Management of fractures of the dens (odontoid process). *J bone Jt surgery Am*. 1980;62(3):482-486.
9. Joaquim AF, Patel A a. Surgical treatment of Type II odontoid fractures: anterior odontoid screw fixation or posterior cervical instrumented fusion? *Neurosurg Focus*. 2015;38(4):1-6.
10. Vasudevan K, Grossberg JA, Spader HS, Torabi R, Oyelese AA. Age increases the risk of immediate postoperative dysphagia and pneumonia after odontoid screw fixation. *Clin Neurol Neurosurg*. 2014;126:185-189.
11. Harms J, Melcher RP. Posterior C1-C2 fusion with polyaxial screw and rod fixation. *Spine*

(Phila Pa 1976). 2001;26(22):2467-2471.

12. Chapman J, Smith JS, Kopjar B, et al. The AOSpine North America geriatric odontoid fracture study. *Spine (Phila Pa 1976)*. 2013;38(13):1098-1104.

13. Kazan S, Tuncer R, Sindel M. Percutaneous anterior odontoid screw fixation technique: A new instrument and a cadaveric study. *Acta Neurochir (Wien)*. 1999;141:521-524.

14. Magerl F, Seemann PS. *Stable Posterior Fusion of the Atlas and Axis by Transarticular Screw Fixation*.; 1987.

15. Taghva A, Attenello FJ, Zada G, Khalessi AA, Hsieh PC. Minimally invasive posterior atlantoaxial fusion: A cadaveric and clinical feasibility study. *World Neurosurg*. 2013;80(3):414-421.

16. Kelly BP, Glaser JA, DiAngelo DJ. Biomechanical comparison of a novel C1 posterior locking plate with the harms technique in a C1-C2 fixation model. *Spine (Phila Pa 1976)*. 2008;33(24):920-925.

17. Hu Y, Gu Y-J, He X-F, et al. Biomechanical evaluation of stability and three-dimensional movements of the atlantoaxial joint after artificial atlanto-odontoid joint arthroplasty. *Orthop Surg*. 2010;2(2):111-118.

18. Chen J, Zhou F, Ni B, et al. New posterior atlantoaxial restricted nonfusion fixation for atlantoaxial instability. *Neurosurgery*. 2015;0(0):1-7.

19. Panjabi MM. Cervical spine models for biomechanical research. *Spine (Phila Pa 1976)*. 1998;23(24):2684-2700.

20. Cai X-H, Liu Z-C, Yu Y, Zhang M-C, Huang W-B. Evaluation of biomechanical properties of anterior atlantoaxial transarticular locking plate system using three-dimensional finite element analysis. *Eur Spine J*. 2013;22:2686-2694.

21. Cai X, Yu Y, Liu Z, Zhang M, Huang W. Three-dimensional finite element analysis of occipitocervical fixation using an anterior occiput-to-axis locking plate system: a pilot study. *Spine J*. 2014;14(8):1399-1409.
22. Zhang B-C, Liu H, Cai X-H, et al. Biomechanical comparison of a novel transoral atlantoaxial anchored cage with established fixation technique - a finite element analysis. *BMC Musculoskelet Disord*. 2015;16:261-272.
23. Panzer MB, Fice JB, Cronin DS. Cervical spine response in frontal crash. *Med Eng Phys*. 2011;33(9):1147-1159.
24. Meyer F, Bourdet N, Deck C, Willinger R, Raul JS. Human neck finite element model development and validation against original experimental data. *Stapp Car Crash J*. 2004;48(11):177-206.
25. Brolin K, Halldin P. Development of a finite element model of the upper cervical spine and a parameter study of ligament characteristics. *Spine (Phila Pa 1976)*. 2004;29(4):376-385.
26. Zhang QH, Ng WN. Development and validation of a C0–C7 FE complex for biomechanical study. *J Biomech Eng*. 2005;127(5):729-735.
27. Cronin DS, Fice JB, Dewit JA, Moulton J. Upper cervical spine kinematic response and injury prediction. In: *IRCOBI Conference*. ; 2012:225-234.
28. Gayzik FS, Moreno DP, Vavalle NA, Rhyne AC, Stitzel JD. Development of a full human body finite element model for blunt injury prediction utilizing a multi-modality medical imaging protocol. In: *12th International LS-DYNA Users Conference*. ; 2012:1-14.
29. Nightingale RW, Winkelstein BA, Knaub KE, Richardson WJ, Luck JF, Myers BS. Comparative strengths and structural properties of the upper and lower cervical spine in

flexion and extension. *J Biomech*. 2002;35(6):725-732.

30. Dibb AT, Nightingale RW, Luck JF, Chancey VC, Fronheiser LE, Myers BS. Tension and combined tension-extension structural response and tolerance properties of the human male ligamentous cervical spine. *J Biomech Eng Eng*. 2009;131(8):81008-1 - 11.

31. Panjabi MM, Dvorak J, Crisco JJ, Oda T, Wang P, Grob D. Effects of alar ligament transection on upper cervical spine rotation. *J Orthop Res*. 1991;9(4):584-593.

32. Panzer MB, Cronin DS. C4-C5 segment finite element model development, validation, and load-sharing investigation. *J Biomech*. 2009;42:480-490.

33. DeWit JA, Cronin DS. Cervical spine segment finite element model for traumatic injury prediction. *J Mech Behav Biomed Mater*. 2012;10:138-150.

34. Mattucci SFE, Moulton JA, Chandrashekar N, Cronin DS. Strain rate dependent properties of human craniovertebral ligaments. *J Mech Behav Biomed Mater*. 2013;23:71-79.

35. Crisco JJ, Oda T, Panjabi MM, Bueff HU, Dvorák J, Grob D. Transections of the C1-C2 joint capsular ligaments in the cadaveric spine. *Spine (Phila Pa 1976)*. 1991;16(10):474-479.

36. Shateri H, Cronin DS. Out-of-position rear impact tissue-level investigation using detailed finite element neck model. *Traffic Inj Prev*. 2015;16(7):698-708.

37. Stander N, Roux W, Goel T, Eggleston T, Craig K. *LS-OPT User's Manual - a Design Optimization and Probabilistic Analysis Tool for the Engineering Analyst*. Livermore, CA; 2012.

38. Panjabi M, Dvorak J, Crisco III J, Oda T, Hilibrand A, Grob D. Flexion, extension, and lateral bending of the upper cervical spine in Response to alar ligament transections. *J*

Spinal Disord. 1991;4(2):157-167.

39. Panjabi M, Dvorak J, Duranceau J, Yamamoto I. Three dimensional movements of the upper cervical spine. *SPIE*. 1988;1030:370-377.

40. Panjabi MM, Crisco J, Vasavada A, et al. Mechanical properties of the human cervical spine as shown by three-dimensional load-displacement curves. *Spine (Phila Pa 1976)*. 2001;26(24):2692-2700.

41. Du J, Aichmair A, Kueper J, Wright T, Lebl D. Biomechanical analysis of screw constructs for atlantoaxial fixation in cadavers: a systematic review and meta-analysis. *J Neurosurg*. 2015;22(2):151-161.

42. Gorek J, Acaroglu E, Berven S, Yousef A, Puttlitz CM. Constructs incorporating intralaminar C2 screws provide rigid stability for atlantoaxial fixation. *Spine (Phila Pa 1976)*. 2005;30(13):1513-1518.

43. Ma X-Y, Yin Q-S, Wu Z-H, et al. C1 pedicle screws versus C1 lateral mass screws: comparisons of pullout strengths and biomechanical stabilities. *Spine (Phila Pa 1976)*. 2009;34(4):371-377.

44. Robertson PA, Tsitsopoulos PP, Voronov LI, Havey RM, Patwardhan AG. Biomechanical investigation of a novel integrated device for intra-articular stabilization of the C1-C2 (atlantoaxial) joint. *Spine J*. 2012;12(2):136-142.